Advection of a magnetic field by a turbulent swirling flow

P. Odier, J.-F. Pinton, and S. Fauve*
Ecole Normale Supérieure de Lyon, CNRS URA 1325, 69364 Lyon, France

(Received 6 July 1998)

We study the magnetic field fluctuations generated by a turbulent swirling flow in the presence of an externally applied magnetic field. We show that the spectra of local magnetic field fluctuations have a region of power law scaling which is interpreted in terms of Kolmogorov's model of turbulent velocity fluctuations. We also discuss the mean and rms values of the magnetic field induced by the velocity gradients. [S1063-651X(98)08312-3]

PACS number(s): 47.65.+a, 47.27.−i

We report an experimental study of the magnetic field fluctuations generated in a turbulent flow of liquid gallium, in the presence of an externally applied field. We consider the case of a weak "seed" field $\vec{B}_0$, so that the Lorentz forces do not modify the flow [1]. The velocity gradients induce magnetic field fluctuations $\vec{b}$ at all scales, the description of which pertains to the dynamics of a "passive vector" in turbulence, in analogy to the passive scalar case [2]. However, this passive vector dynamics involves stretching of magnetic field lines by velocity gradients, analogous to stretching of vorticity lines, and is thus at an intermediate level of complexity between passive scalar advection and fully developed turbulence. In particular, stretching of magnetic field lines by velocity gradients may overcome Joule dissipation and generate a large scale magnetic field by amplification of weak initial disturbances—this is the dynamo effect, which is at the origin of the magnetic field of the earth and of many astrophysical objects [3,4]. Our first motivation is to study the statistical properties of the fluctuating magnetic field; incidentally we show that it can be used as a probe of the turbulent velocity gradients. There exist almost no experimental studies of this problem, i.e., the effect of a flow of liquid metal on an externally applied magnetic field [5,6], whereas much research has been devoted to the modification turbulence by a strong Lorentz force. Our second motivation is to use the field $\vec{b}$ generated by velocity gradients as a response function of the turbulent flow to the applied field $\vec{B}_0$, in order to obtain insights into the stretching mechanisms believed to be at the origin of the dynamo effect. We use the flow created in the gap between two coaxial rotating disks, the von Kármán swirling flow, as it is known to involve strong stretching by velocity gradients [7]. This leads to an amplification of intense vorticity both for counter-rotating [8] or corotating disks [9]. One may thus expect a similar efficiency for the amplification of magnetic field fluctuations because of the $\vec{\omega}$-$\vec{b}$ analogy [3]. In addition, this flow possesses many features, such as differential rotation or poloidal and toroidal mean flow components, which are known to favor dynamo action [3].

Our experimental setup is schematically shown in Fig. 1. Two 11-kW ac motors are used to drive the disks (radius $R = 10$ cm) at a constant frequency Ω, adjustable in the range 5–50 Hz. The enclosing cylindrical vessel has a volume of 5.5 liters. It is filled with liquid gallium (density $\rho = 6.09 \times 10^3$ kg m^{-3}), chosen for its high electrical conductivity ($\sigma = 3.68 \times 10^6\ \Omega^{-1}$ m^{-1}). Its kinematic viscosity is $\nu = 3.1 \times 10^{-7}$ m^2 s^{-1}. The integral kinematic and magnetic Reynolds numbers of the flow are defined as $R_e = 2\pi R^2\Omega/\nu \in [10^6, 10^7]$ and $R_m = 2\pi\mu_0\sigma R^2\Omega \in [1.3, 15]$. Note that, as in all liquid metals, the magnetic Prandtl number $P_m = \mu_0\sigma\nu$ is very small ($\sim 10^{-6}$). Thus the flow is strongly turbulent (R_e is large) even at moderate values of R_m, for which interesting dynamics of the magnetic field are expected. The surfaces of the disks bear an etched pattern in the form of squares 1 mm thick. The purpose of this artificial rugosity is to ensure an inertial entrainment of the fluid. In this case the rms value of the velocity fluctuations is proportional to (and equal to about a tenth of) the disk's rim speed: The flow power consumption P then scales as Ω^3 [10]. Measurements yield $P = K(\rho R^5 \Omega^3)$, with $K = 13.3 \pm 0.1$, a numerical constant independent of the Reynolds number. It is dissipated into heat by the turbulent motion and drained off by the cooling circuits located behind the disks. For each run at a fixed rotation rate, the flow is kept at a constant temperature $\theta \in [40\ °C, 80\ °C]$. Two pairs of Helmholtz coils are set to produce an external field B_0 up to 40 G, either parallel or perpendicular to the rotation axis. Magnetic measurements are performed inside the vessel using directional and temperature compensated Hall probes with a Bell 9905 gauss-

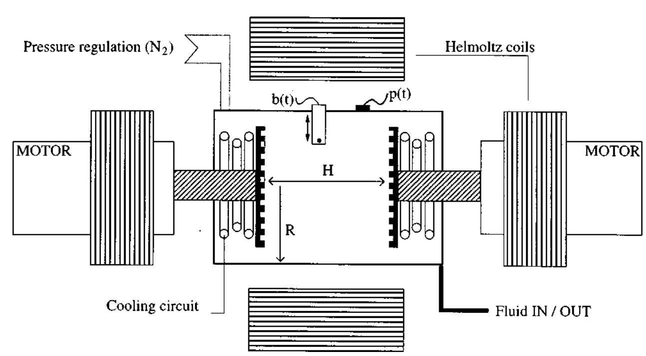

FIG. 1. Experimental setup (not to scale). $R = 10$ cm, $H = 10$ cm. The magnetic Hall probe is located in the median plane, at a variable distance d from the rotation axis.

*Present address: Ecole Normale Supérieure, CNRS URA 1306, 75231 Paris, France

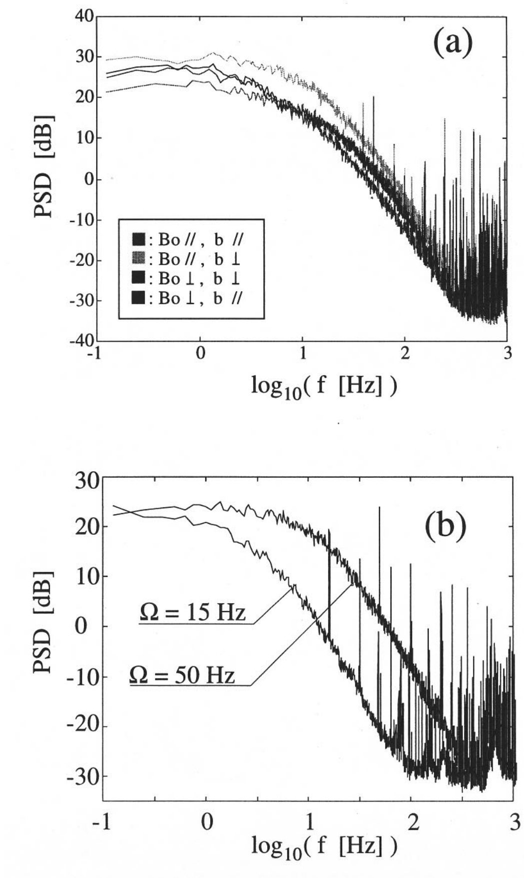

FIG. 2. (a) Magnetic spectra for different orientations ($\vec{B}_0, \vec{b}$) with respect to the rotation axis of the applied and induced fields, $\Omega = 40$ Hz; $R_m = 10.8$; probe at $d = 1$ cm from the wall. (b) Magnetic spectra for $R_m = 3.5$ and $R_m = 15$, for the field component parallel to the rotation axis. $\vec{B}_0$ is also axial.

meter, the spatial resolution is 3 mm, with a frequency range of 50 kHz in the ac mode or 400 Hz in the dc mode. Pressure measurements are performed with an acceleration compensated transducer PCB H112A21, 5 mm in diameter, mounted flush with the lateral wall [11].

When a steady magnetic field is applied on the flow, an induced field is produced as a result of stretching by the local velocity gradients. As the flow is fully turbulent, the velocity gradients follow scaling laws in a range of scales—the so-called inertial domain of turbulence [2]. One may thus expect scaling properties for the magnetic field fluctuations. Figure 2(a) shows typical power spectra (in time) of magnetic field fluctuations. The measurements are made at $R_m = 10.8$ with the Hall probe placed inside the flow; the curves correspond to different orientations of the applied field $\vec{B}_0$ and induced component $\vec{b}$. They are quite similar, with first a flat frequency region followed by a steep cutoff which displays an algebraic decay $\tilde{b}^2(f) \propto f^{-\alpha}$ (the discrete lines in the spectrum corespond to noise generated by the electric motors driving the disks). When comparing magnetic spectra recorded at increasing rotation rates (and hence magnetic Reynolds number)—see Fig. 2(b)—one observes that this behavior is preserved. The transition between the flat spectral region and the power law one occurs for a frequency of the order of Ω, i.e., the integral time scale of the flow. The

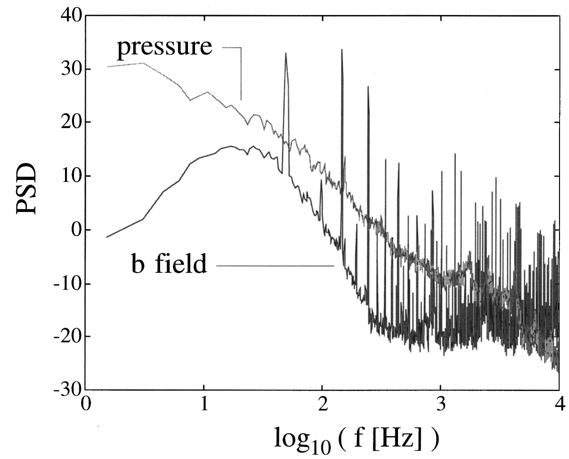

FIG. 3. Comparison of magnetic and pressure spectra, at $R_m = 10.8$. The pressure is measured at the lateral wall. The low frequency cutoff in the magnetic spectrum is due to the ac filtering of the gaussmeter.

scaling region also widens with increasing R_m; it is always larger than a decade. Note that this is a lower bound since our measurements are limited by the amplitude resolution of the Hall probes; the actual extent of the scaling zone of the magnetic fluctuations may be larger. In Fig. 3 we compare it with the scaling domain of pressure fluctuations measured at the flow wall. It can bee seen there that it lies in the domain where the pressure fluctuations also follow a power law, i.e., in the inertial range of the velocity field [11]. We thus observe a scaling behavior of the magnetic field fluctuations $\tilde{b}^2(f) \propto f^{-\alpha}$, in the inertial range of turbulence. Measurements for all orientations and accessible values of R_m yield $\alpha = 3.7 \pm 0.2$.

These results can be understood as follows. In the presence of a uniform and constant applied field $\vec{B}_0$, magnetic field perturbations $\vec{b}$ are governed by the equations [3]:

$$(\partial_t + \vec{u} \cdot \vec{\nabla})\vec{b} = [(\vec{b} + \vec{B}_0) \cdot \vec{\nabla}]\vec{u} + \lambda \Delta \vec{b}, \qquad \vec{\nabla} \cdot \vec{b} = 0. \tag{1}$$

Since the magnetic diffusivity ($\lambda = 1/\mu_0 \sigma$) is orders of magnitude larger than the kinematic viscosity, $\vec{b}$ adiabatically follows $\vec{u}$. In this ''quasistatic'' approximation [12,13], one has, to leading order

$$\lambda \Delta \vec{b} \approx -(\vec{B}_0 \cdot \vec{\nabla})\vec{u}, \tag{2}$$

provided that the induced field is much smaller than the applied ones, as is well verified in our experiment. Thus $\vec{b}$ obeys a Poisson equation—this is analogous to the pressure field albeit second order derivatives of the velocity field are involved in the later case. Keeping in mind that the flow is not modified by $\vec{B}_0$, Eq. (2) and a dimensional analysis in the framework of Kolmogorov phenomenology then leads to

$$\tilde{b}^2(k) \propto k^{-2} \tilde{u}^2(k) \sim k^{-11/3} \tag{3}$$

in the inertial range. This behavior, predicted by Golytsin [12] and Moffatt [13] for turbulent magneto hydrodynamics

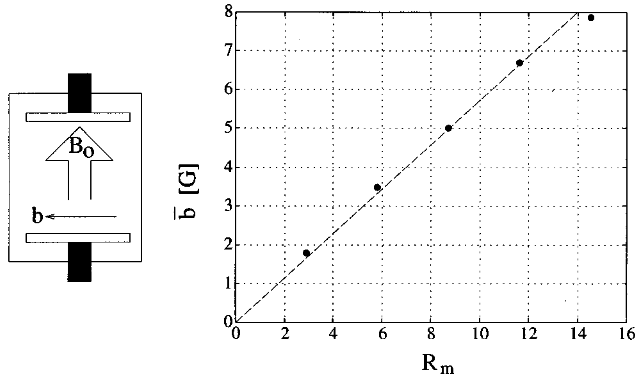

FIG. 4. Azimutal component of the induced field for an applied field of 33 G applied in the direction of the rotation axis.

(MHD) flows at very small magnetic Prandtl number, is consistent with our measurements, providing Taylor's hypothesis may be used [14],

Note that, when eddy-damped quasinormal Markovian (EDQNM) closures are applied to MHD equations, the relation $\tilde{b}^2(k) \propto k^{-2}\tilde{u}^2(k)$ between kinetic and magnetic energy subsists when the magnetic field is generated by the dynamo effect, although both spectra are steeper because of the effect of the Lorentz force [15]. We thus find that the magnetic energy is confined to large scales of the flow, the small scale fluctuations being rapidly damped through the combined action of stretching and Joule dissipation. The similarity of the high frequency regions of the magnetic spectra in Fig. 2(a) shows that the small scale velocity gradients are fairly isotropic, in agreement with Kolmogorov phenomenology; conversely, the differences in the low frequency parts are ascribed to the effects of large scale gradients which are far from being isotropic in this flow. We also emphasize that although the curves in Figs. 2 and 3 correspond to a measurement near the lateral wall at $R_m \sim 11$, these features are found for all values of R_m and positions d of the probe inside the flow.

We now consider the temporal average, $\overline{b}$ of the magnetic field $\vec{b}$. Equation (2) yields:

$$\overline{b(\vec{r})} \approx g \star (\vec{B}_0 \cdot \vec{\nabla})\vec{u}, \tag{4}$$

where g is a Green function (equal to the free space one only for insulating boundary conditions at the vessel walls, and the $\star$ denotes the convolution of functions). Equation (4) is the leading order term for the distortion of the magnetic field lines; it is due to the nonuniformity of the flow along $\vec{B}_0$ and varies linearly with R_m at small R_m [1,3]. This is evidenced in Fig. 4, where the azimutal component of the induced field is plotted against R_m, for an applied field parallel to the rotation axis z. Here an azimutal component b_θ is induced by the stretching term $\partial_z u_\theta$, i.e., by differential rotation (the disks rotate in opposite directions).

Note here that we have checked that $\overline{b}$ is linear as a function of B_0, even at a small rotation rate of the disks. This shows that the velocity field, $\vec{u}$, is not affected by the Lorentz force, in agreement with the small value of the interaction parameter $\sigma B_0^2 R/\rho u$ (the ratio of Lorentz to pressure forces).

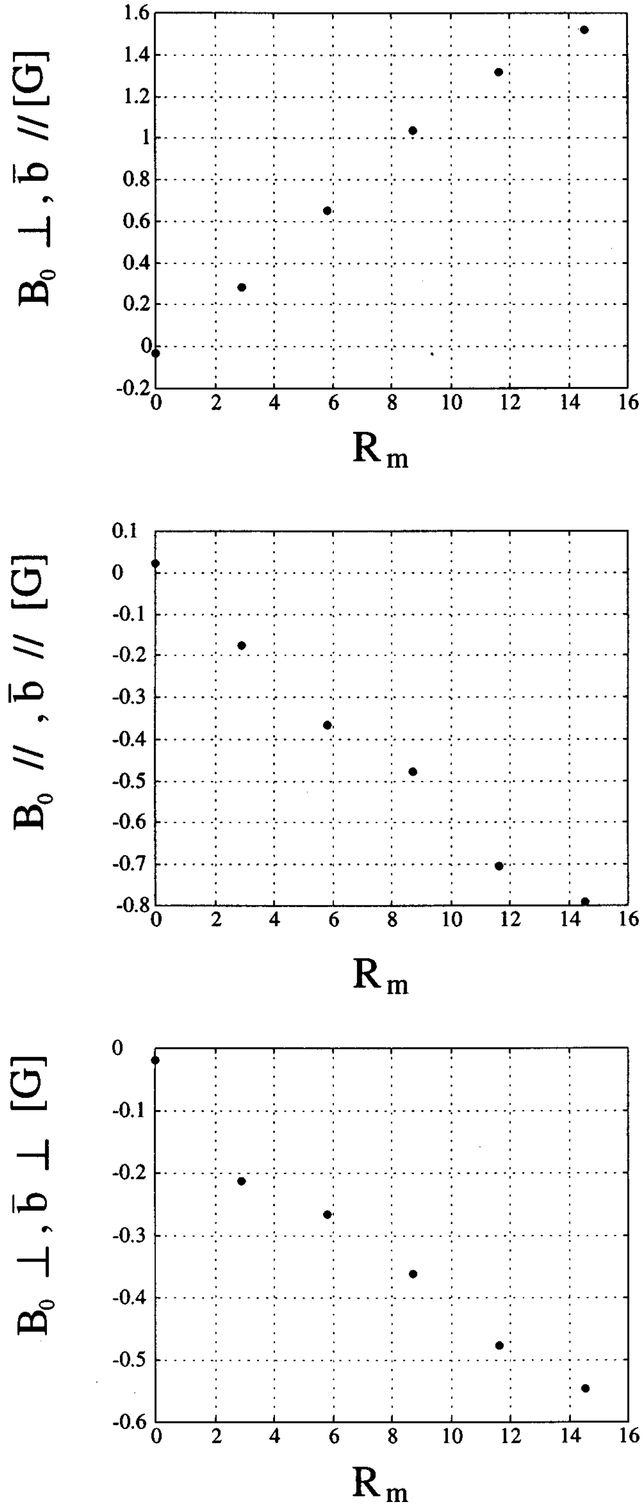

FIG. 5. Average value of the magnetic field for different orientations $(\vec{B}_0, \vec{b})$ with respect to the rotation axis of the applied and induced field.

A similar induction of magnetic field is observed when the applied field is oriented normal to the rotation axis—see Fig. 5. A perpendicular magnetic component (i.e., $\overline{b}$ parallel to the rotation axis) is observed, at every position d of the probe inside the flow. This is due to the nonuniformity in the transverse direction of the axial velocity component. Here again, the amplitude of the induced field varies linearly with

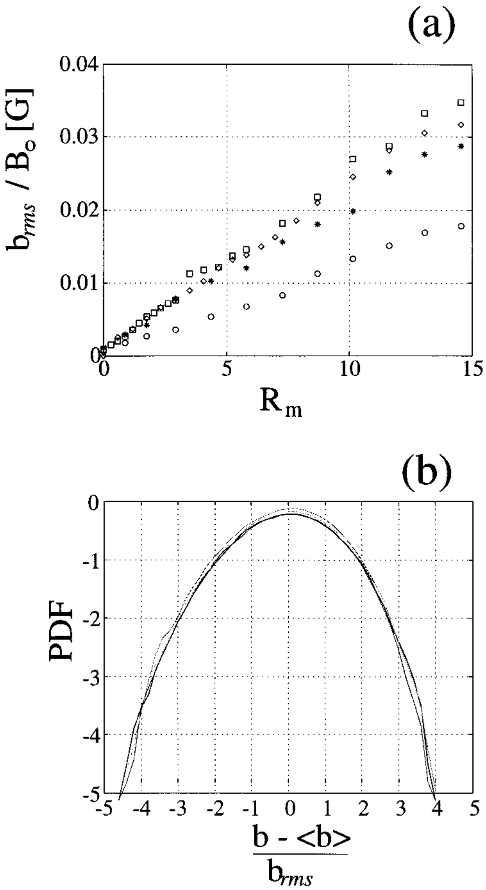

FIG. 6. (a) Evolution of the rms amplitude of the induced magnetic field, for $R_m \in [2,15]$; the respective orientations of the applied field and measured induced components are ($\bigcirc = B_0\|, b\|$), ($\square = B_0\|, b\perp$), ($\diamond = B_0\perp, b\|$, and ($\bigstar = B_0\perp, b\perp$). (b) Corresponding probability density function.

R_m. It is thus seen that the three dimensional structure of the mean flow results in a three-dimensional 3D geometry for the magnetic field induced by the velocity gradients.

Additional information about the velocity gradients is obtained by studying the fluctuations of the induced field. We first observe that $b_{\rm rms}$ varies linearly with R_m—cf. Fig. 6(a)—as expected from Eq. (4). The slopes of $\overline{b}/B_0$ and $b_{\rm rms}/B_0$ as a function of $R_{\rm m}$ are different—see Table I. We attribute this to the fact that whereas the mean value of the induced field $\overline{b}$ is due to the large scale structure of the mean flow, its fluctuations are generated by the turbulent fluctuations. In agreement with previous velocimetry measurements in this type of flow, we observe that the mean velocity gradients are larger spanwise (i.e., for derivatives taken in the transverse direction).

TABLE I. Variation of rms fluctuations of the induced magnetic field, for an applied field of 20 G. The $\|$ and $\perp$ symbols denote the orientations of the applied and induced field with respect to the rotation axis of the disks.

	$B_0\|, b\|$	$B_0\|, b\perp$	$B_0\perp, b\|$	$B_0\perp, b\perp$
$\frac{1}{B_0}\frac{db_{\rm rms}}{dR_m}$	0.0012	0.0024	0.0022	0.0019
$\frac{1}{B_0}\frac{db}{dR_m}$	-0.0016	0.0157	0.0065	-0.0018

Another fact is that b has quasi-Gaussian fluctuations, as shown in Fig. 6(b). This is in sharp contrast with the behavior of pressure fluctuations in turbulent flows, which display asymmetric probability density functions with an exponential tail toward the low values [11]. Note that both fields obey a Poisson equation with a source term involving the velocity gradients. The main difference is that the source term is linear for b, and quadratic for p.

Finally, we discuss the three-dimensional dynamics of the magnetic field in our flow in regard to the dynamo problem. First we observe that differential rotation generates a toroidal field component from a poloidal one; this is an important mechanism for dynamo action [3]. Indeed, this effect is the source of solid rotor dynamos introduced by Herzenberg [13], and shown in the experiment of Lowes and Wilkinson [16]. Second, we observe the induction of an axial field from an applied transverse field. Together, these processes may lead to a nonlinear growth of the magnetic energy. Indeed, starting with $\vec{B}_0$, the large scale velocity gradients generate an induced component $\vec{b}^{(1)}$ with an amplitude $O(B_0 R_m)$; in turn, $\vec{b}^{(1)}$ can be acted upon by the velocity gradients to produce an induced field $\vec{b}^{(2)}$ whose amplitude is now $O(b^{(1)}R_m) \sim O(B_0 R_m^2)$, etc. We note that numerical studies of flows with similar geometries (but different boundary conditions), based on kinematic dynamo calculations [17] or using direct simulation [18], and EDQNM closures of MHD equations [15], show that dynamo action occurs and gives critical values $R_m^c \in [20,50]$ for its onset. Work is underway to operate our flow using liquid sodium as a working fluid; magnetic Reynolds numbers exceeding 80 will be reached.

This experiment was designed with the technical help of Claude Laroche, Djamel Bouraya, and Marc Moulin. We thank Rhône-Poulenc for lending us the gallium. This work was supported by grants from Centre National de la Recherche Scientifique and the French Education and Research Ministery.

[1] P. H. Roberts, *An Introduction to Magnetohydrodynamics* (Longmans, London, 1967).
[2] A. S. Monin and A. M. Yaglom, *Statistical Fluid Mechanics* (MIT Press, Cambridge, MA, 1975).
[3] H. K. Moffatt, *Magnetic Field Generation in Electrically Conducting Fluids* (Cambridge, University Press, Cambridge, 1978).
[4] Ya. B. Zeldovich, A. A. Ruzmaikin, and D. D. Sokoloff, *Magnetic Fields in Astrophysics* (Gordon and Breach, London, 1983).

[5] M. Steenbeck, I. M. Kirko, A. Gailitis, A. P. Klawina, F. Krause, I. J. Laumanis, and O. A. Lielausis, Sov. Phys. Dokl. **13**, 443 (1968).
[6] I. M. Kirko, C. R. Acad. Sci. USSR **257**, 127 (1981).
[7] P. J. Zandbergen and D. Dijkstra, Annu. Rev. Fluid Mech. **19**, 465 (1987), and references therein.
[8] S. Douady, Y. Couder, and M.-E. Brachet, Phys. Rev. Lett. **67**, 983 (1991).
[9] R. Labbé, J.-F. Pinton, and S. Fauve, J. Phys. II **6**, 1099 (1996).
[10] N. Mordant, J.-F. Pinton, and F. Chillà, J. Phys. II **7**, 1 (1997).
[11] S. Fauve, C. Laroche, and B. Castaing, J. Phys. II **3**, 271 (1993).
[12] G. S. Golitsyn, Sov. Phys. Dokl. **5**, 536 (1960).
[13] H. K. Moffatt, J. Fluid Mech. **11**, 625 (1961).
[14] This is certainly correct for the pressure measurements, but less obvious for magnetic fluctuations. A detailed discussion is postponed to a forthcoming paper.
[15] J. Léorat, A. Pouquet, and U. Frisch, J. Fluid Mech. **104**, 419 (1981).
[16] F. J. Lowes and I. Wilkinson (unpublished).
[17] N. L. Dudley and R. W. James, Proc. R. Soc. London, Ser. A **425**, 407 (1989).
[18] C. Nore, M.-E. Brachet, H. Politano, and A. Pouquet, Phys. Plasmas **4**, 1 (1997).